

# Imaging of Primary and Metastatic Pancreatic Cancer Using a Fluorophore-Conjugated Anti-CA19-9 Antibody for Surgical Navigation

Michele McElroy · Sharmeela Kaushal · George A. Luiken · Mark A. Talamini ·  
A. R. Moossa · Robert M. Hoffman · Michael Bouvet

© Société Internationale de Chirurgie 2008

## Abstract

**Background** Despite recent surgical advances, pancreatic cancer remains the fourth leading cause of cancer-related death in the United States. This is due to inaccurate staging and difficulty in achieving negative margins at the time of pancreaticoduodenectomy. CA19-9 is a carbohydrate tumor-associated antigen found in up to 94% of pancreatic adenocarcinomas. In this study we investigate the use of a fluorophore-labeled anti-CA19-9 monoclonal antibody to improve intraoperative visualization of both primary and metastatic tumors in a mouse model of pancreatic cancer. **Methods** A monoclonal antibody specific for CA19-9 was conjugated to a green fluorophore and delivered to tumor-bearing mice as a single intravenous (IV) dose. Intravital fluorescence imaging was used to localize tumor implants 24 h after antibody administration.

**Results** Using fluorescence imaging, the primary tumor was clearly visible at laparotomy, as were small metastatic implants within the liver and spleen and on the peritoneum.

These tumor implants, which were nearly impossible to see using standard bright-field imaging, demonstrated clear fluorescence under LED light excitation. The fluorescence signal within the tumor tissue was maintained for over 3 weeks after a single administration of the labeled antibody. Histologic evaluation of tissue from animals treated with the conjugated anti-CA19-9 antibody likewise revealed strong staining of the tumor cells with minimal background staining of the peritumoral stroma.

**Conclusions** Fluorophore-labeled anti-CA19-9 offers a novel intraoperative imaging technique for enhanced visualization of primary and metastatic tumors in pancreatic cancer when CA19-9 expression is present and may improve intraoperative staging and efficacy of resection.

## Introduction

Pancreatic cancer remains a lethal disease with a 5-year survival rate of less than 5% [1]. Ongoing clinical research has yielded few improvements in our ability to medically treat patients with this disease and surgery remains the only chance of cure for patients with pancreatic cancer [2]. Despite many advances in preoperative patient evaluation and in surgical and critical care [3, 4], pancreatic cancer continues to contribute significantly to cancer-related morbidity and mortality [1]. Due to its late stage at presentation, early metastasis, and the characteristic stromal reaction in the surrounding pancreatic tissue [5], appropriate intraoperative staging and successful resection with clear margins remain a challenge [2]. Unfortunately, for some patients inadequate preoperative and intraoperative identification of tumor can lead to unnecessary laparotomy and possibly incomplete resection at the time of surgery

---

Presented at the International Surgical Week, Montreal, Quebec, Canada, August 26-30, 2007, in the Lloyd M. Nyhus Prize Session

---

M. McElroy · S. Kaushal · M. A. Talamini ·  
A. R. Moossa · R. M. Hoffman · M. Bouvet (✉)  
Department of Surgery, University of California, San Diego,  
California 92093, USA  
e-mail: mbouvet@ucsd.edu

R. M. Hoffman  
AntiCancer, Inc, San Diego, California, USA

G. A. Luiken  
OncoFluor, Inc, San Diego, California, USA

M. Bouvet  
UCSD Moores Cancer Center, 3855 Health Sciences Drive, Mail  
Code 0987, La Jolla, CA 92093-0987, USA

[3]. Clearly, strategies to improve both intraoperative staging and to facilitate complete tumor resection would benefit patients.

Tumor-associated antigens have been utilized for some time in serologic tests both as an aid in early diagnosis and as a way to monitor known cancer patients for recurrence or progression of disease [6]. CA19-9 is one such antigen which is associated with several different types of gastrointestinal cancers but which has become the gold standard for serologic testing of pancreatic cancer. In addition to its secretion into the bloodstream, CA19-9 has been shown to be present within the cytoplasm and on the membrane of pancreatic adenocarcinoma cells [7, 8], making it a promising potential antigen for targeted tumor imaging.

In this study we have investigated the possibility of combining the specificity of a monoclonal antibody targeted to the tumor-associated antigen CA19-9 with the power of fluorescence imaging in order to facilitate the visualization of both primary and metastatic pancreatic cancer in a mouse model.

## Material and methods

### Cell culture

The human pancreatic cancer cell lines XPA-1, XPA-3, XPA-4, BxPc-3, and ASPC-1 were maintained in RPMI 1640. Panc-1, Colo-357, Mia Paca-2, and FG were maintained in DMEM, and CaPan-1 and CFPAC were grown in IMDM. All media was supplemented with 10% fetal calf serum (FCS) (Hyclone, Logan, UT), penicillin/streptomycin (Gibco-BRL, Grand Island, NY), L-glutamine (Gibco-BRL), MEM nonessential amino acids (Gibco-BRL), sodium bicarbonate (Cellgro, Herndon, VA), and sodium pyruvate (Gibco-BRL). All cells were cultured at 37°C with 5% CO<sub>2</sub>.

### Conjugation of antibody to fluorophore

Monoclonal antibody specific for CA19-9 was purchased from Biodesign International (Saco, ME). The antibody was labeled with the AlexaFluor 488 Protein Labeling Kit (Molecular Probes Inc., Eugene, OR) according to the manufacturer's instructions. Briefly, the monoclonal antibody was reconstituted at 1 mg/ml in 0.1 M sodium bicarbonate. One hundred microliters of the 1 mg/ml solution were added to the reactive dye and allowed to incubate for 1 h at room temperature, then overnight at 4°C. The conjugated antibody was then separated from the remaining unconjugated dye on a purification column by centrifugation. Antibody and dye concentrations in the final

sample were determined using spectrophotometric absorbance.

### In vitro fluorescent imaging

All cell lines were plated in 96-well plates at  $1 \times 10^5$  cells per well. After 48-h culture in appropriate media, the cells had reached confluence and were incubated with 1 µg of conjugated anti-CA19-9 antibody for 4 h at 37°C, then washed three times with phosphate-buffered saline (PBS). Cells were imaged with an inverted Nikon DE-300 fluorescence microscope and Spot camera RD. The images were then analyzed using Metamorph Software (Universal Imaging Corporation, West Chester, PA). For repeated sequential imaging the cells were washed once with PBS and the media was replaced each day prior to imaging.

### Animal care

Athymic *nu/nu* nude mice between 4 and 6 weeks of age were maintained in a barrier facility on high-efficiency particulate air (HEPA)-filtered racks. The animals were fed with autoclaved laboratory rodent diet (Teckland LM-485; Western Research Products, Orange, CA). All surgical procedures and intravital imaging were performed with the animals anesthetized by intramuscular injection of 0.02 ml of a solution of 50% ketamine, 38% xylazine, and 12% acepromazine maleate. All animal studies were conducted in accordance with the principles and procedures outlined in the NIH Guide for the Care and Use of Animals.

### Subcutaneous tumor cell implantation

The human pancreatic cancer cell line BxPC3 was harvested by trypsinization and washed three times with cold serum-free medium. BxPC3 cells ( $1 \times 10^6$ ) were injected subcutaneously in a total volume of 100 µl of serum-free media using a 1-ml 27G latex-free syringe (Becton, Dickinson, Franklin Lakes, NJ) within 30 min of harvesting. Antibody administration and intravital imaging were performed 10 days after injection of the tumor cells. After the completion of imaging the flank tumors were excised for ex vivo measurements of weight and volume.

### Orthotopic tumor implantation

Orthotopic human pancreatic cancer xenografts from the pancreatic cancer cell line BxPC3 were established in nude

mice by surgical orthotopic implantation (SOI) as previously described [9–11]. Subcutaneous BxPC3 tumors in the exponential growth phase were harvested and sectioned into 1-mm<sup>3</sup> pieces in RPMI medium. The animals were anesthetized as described previously and a small transverse incision was then made in the left lateral flank through the skin and peritoneum. The tail of the pancreas was exposed and a 1-mm<sup>3</sup> tumor fragment was sutured to the pancreatic tail using a single 8-0 nylon surgical suture (US Surgical, Norwalk, CT). The pancreas was then returned to the abdomen and the peritoneum and skin were closed using 6-0 polysorb surgical suture (US Surgical). Antibody administration and intravital imaging were performed 2 weeks following SOI.

### Experimental metastasis tumor models

For the splenic and liver metastasis models, BxPC3 cells were harvested by trypsinization and washed three times in serum-free media. The cells were resuspended in a 1:1 mixture of serum-free media and matrigel (BD Biosciences, Bradford, MA). Cells ( $2 \times 10^5$ ) in 20  $\mu$ l final volume were injected directly into the spleen or liver parenchyma using a 50- $\mu$ l Hamilton syringe (Hamilton Company, Reno, NV) within 30 min of cell harvesting. For the peritoneal implants,  $1 \times 10^6$  BxPC3 cells resuspended in 100  $\mu$ l serum-free media were injected directly into the intraperitoneal cavity. Antibody administration and intravital imaging were performed 1 week following tumor cell implantation for the splenic and peritoneal metastases models and 2 weeks following implantation for the liver metastasis model.

### Antibody delivery

Animals were given a single IV injection of labeled CA19-9 antibody diluted in PBS to a final volume of 100  $\mu$ l. The fluorophore conjugated anti-CA19-9 antibody was injected via the tail vein. For the dose-response experiment, the antibody dose ranged from 7.5 to 100  $\mu$ g. For the in vivo time course of the orthotopic model and the experimental metastatic models, the dose given was 75  $\mu$ g. All animals were first anesthetized and imaged 24 h after administration of the antibody.

### Animal imaging

Mice were imaged using the Olympus OV100 Small Animal Imaging System (Olympus Corp., Tokyo, Japan), containing an MT-20 light source (Olympus Biosystems,

Planegg, Germany) and DP70 CCD camera (Olympus Corp.) [12]. All images were analyzed using Image-J (National Institutes of Health, Bethesda, MD) and were processed for contrast and brightness with the use of Photoshop Elements 4 (Adobe Systems Inc., San Jose, CA).

### Histology

Tumor samples were surgically removed en bloc with surrounding tissue following in vivo imaging. These tissue samples were then frozen in Tissue-Tek O.C.T. compound (Sakura Fintek, Torrance, CA) and sectioned on a microtome. Thick (15  $\mu$ m) sections were prepared without fixation for fluorescence microscopy and thin (8  $\mu$ m) sections for H&E staining and standard light microscopy. All slides were imaged using an inverted Nikon DE-300 fluorescent microscope and Spot camera RD. All images were analyzed using Image-J (National Institutes of Health, Bethesda, MD) and were processed for contrast and brightness with the use of Photoshop Elements 4 (Adobe Systems Inc., San Jose, CA).

### Results

Established human pancreatic cancer cell lines were evaluated in vitro for presence and duration of CA19-9 expression (Fig. 1). Several different cell lines, including XPA-1, XPA-3, XPA-4, BxPC-3, ASPC-1, Panc-1, Colo-357, Mia Paca-2, FG, CaPan-1, and CFPAC, were grown in culture and stained with our conjugated CA19-9 antibody as described. Staining of these human pancreatic cancer cell lines in culture revealed positive expression of CA19-9 in 3 of 11 lines tested, including CFPAC, BxPC-3, and PANC-1 (data not shown). In vitro staining of BxPC3 cells revealed a positive signal for up to 5 days after a single application of conjugated antibody, with a gradual decrease in signal intensity over time.

In vivo dosing of conjugated antibody revealed predictable increases in tumor fluorescence intensity with increasing antibody dose in the subcutaneous tumor model (Fig. 2). Nude mice with small (1-2-mm diameter) subcutaneous flank tumors were given a single IV administration of conjugated CA19-9 in doses ranging from 7.5 to 100  $\mu$ g per animal. Each animal was imaged 24 h after antibody administration using the Olympus OV-100 Small Animal Imaging System. Tumors were imaged both through the skin and via a small skin flap. After imaging, the tumors were harvested, measured, and weighed. The antibody dose was adjusted for tumor weight. With doses as low as 12.5  $\mu$ g (0.5  $\mu$ g Ab/mg

**Fig. 1** In vitro fluorescence intensity over time. The human pancreatic cancer cell line BxPC3 was plated at  $10^5$  cells per well in a 96-well plate. Forty-eight hours later the confluent monolayer of cells was incubated with conjugated monoclonal CA19-9. The cells were then washed and imaged using an inverted fluorescence microscope at  $100\times$  magnification. Each day the cells were washed and the medium was replaced prior to imaging. Wells were evaluated in triplicate. The fluorescence signal remained present within the monolayer for 5 days

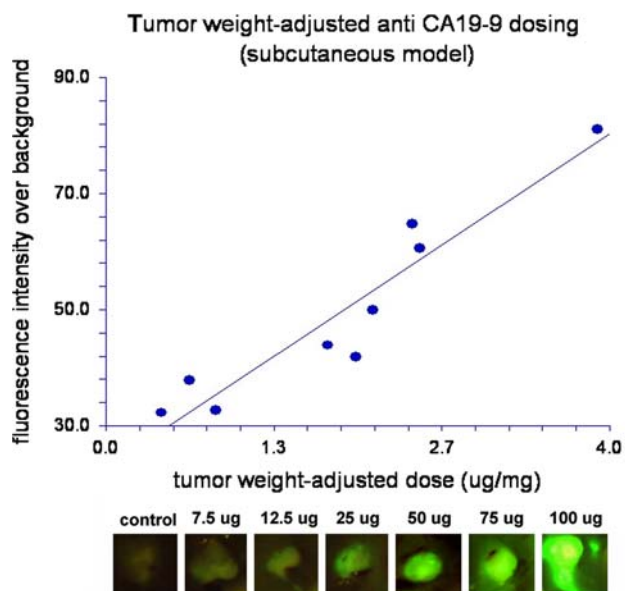
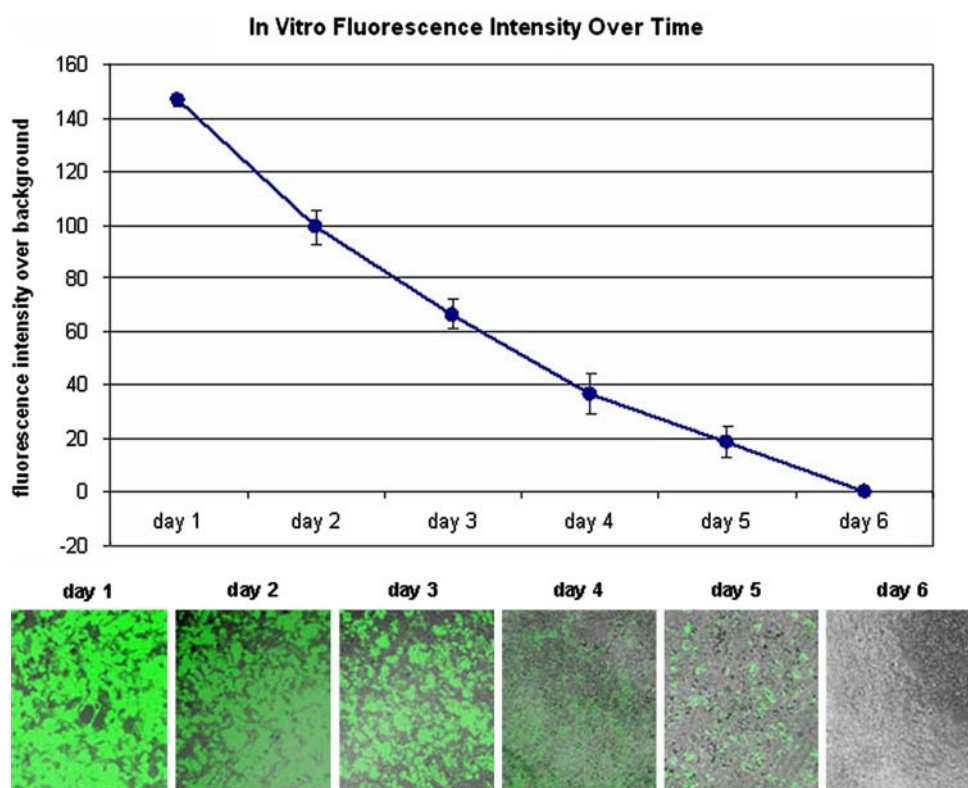


**Fig. 2** CA19-9 dose-response. Athymic nude mice with small (1-2-mm diameter) flank tumors were given a single intravenous dose of CA19-9 ranging from 7.5 to 100  $\mu\text{g}$ . All animals were imaged 24 h later and the fluorescence intensity of the tumors was measured using Image-J software. Tumor fluorescence was visible above background at 12.5  $\mu\text{g}$  and all higher doses. Increasing antibody dose correlated with increasing fluorescence intensity across all doses given ( $n = 11$ )

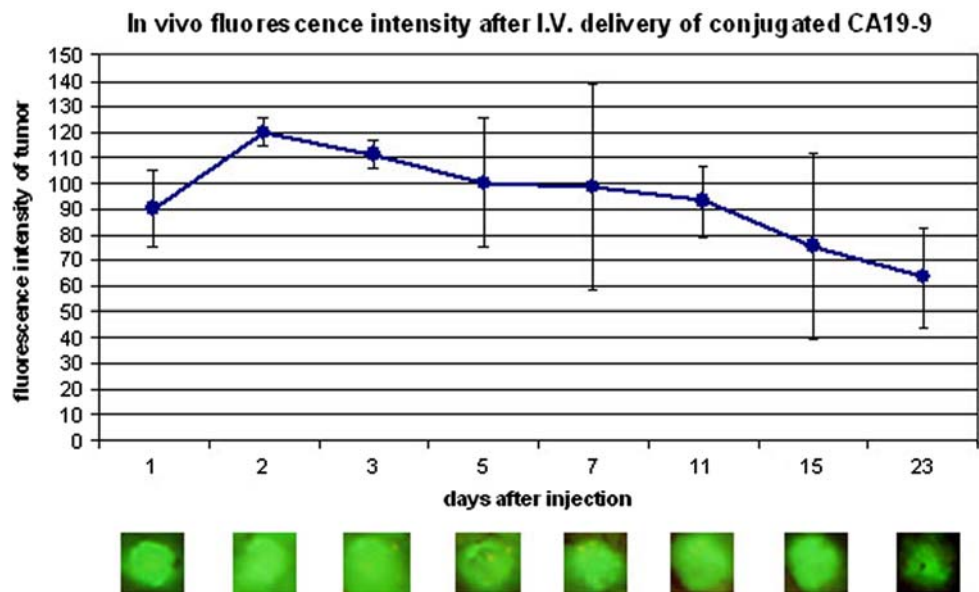
tumor), the tumors were clearly visible above the background autofluorescence. In addition, the fluorescence intensity of the tumors increased in a linear fashion with

increasing dose of antibody, with no short-term toxicity noted at any dose tested.

The fluorescence signal within the tumor remained stable for over 3 weeks following a single dose of conjugated antibody (Fig. 3). Nude mice with small flank tumors were given a single dose of 75  $\mu\text{g}$  of conjugated CA19-9 antibody. The animals were imaged at 1, 2, 3, 5, 7, 9, 11, 13, 15, 19, and 23 days after antibody delivery. Tumors were visualized via a small skin flap elevated at each time point and were imaged using the Olympus OV-100 Small Animal Imaging System. All tumors demonstrated bright green fluorescence at 24 h after antibody delivery, with the signal persisting to day 23 postinjection. Long-term follow-up of these animals revealed no toxic effects of the systemic delivery of conjugated antibody.

Administration of conjugated CA19-9 to animals with small orthotopic pancreatic tumors facilitated visualization of the primary tumor at laparotomy (Fig. 4). Two weeks following surgical orthotopic implantation of a small (1  $\text{mm}^3$ ) fragment of solid BxPC3 tumor, animals were given a single dose of 75  $\mu\text{g}$  of conjugated CA19-9. Twenty-four hours later the mice were anesthetized and the pancreas was visualized via a midline laparotomy incision. Small tumors were virtually unidentifiable under standard bright-field imaging (Fig. 4A) but were clearly visible using fluorescence imaging (Fig. 4C). In contrast, mice with small orthotopic tumors that were not given the antibody had tumors that were difficult to localize under

**Fig. 3** Time course of in vivo fluorescence intensity after intravenous delivery of conjugated CA19-9. Athymic nude mice with small (1–2-mm diameter) flank tumors were given a single intravenous dose of 75  $\mu$ g of CA19-9. The animals were anesthetized and the tumors were imaged via a skin flap 1, 2, 3, 5, 7, 9, 11, 13, 15, 19, and 23 days after antibody delivery. The fluorescence signal remained present for over 3 weeks after antibody administration ( $n = 3$ )

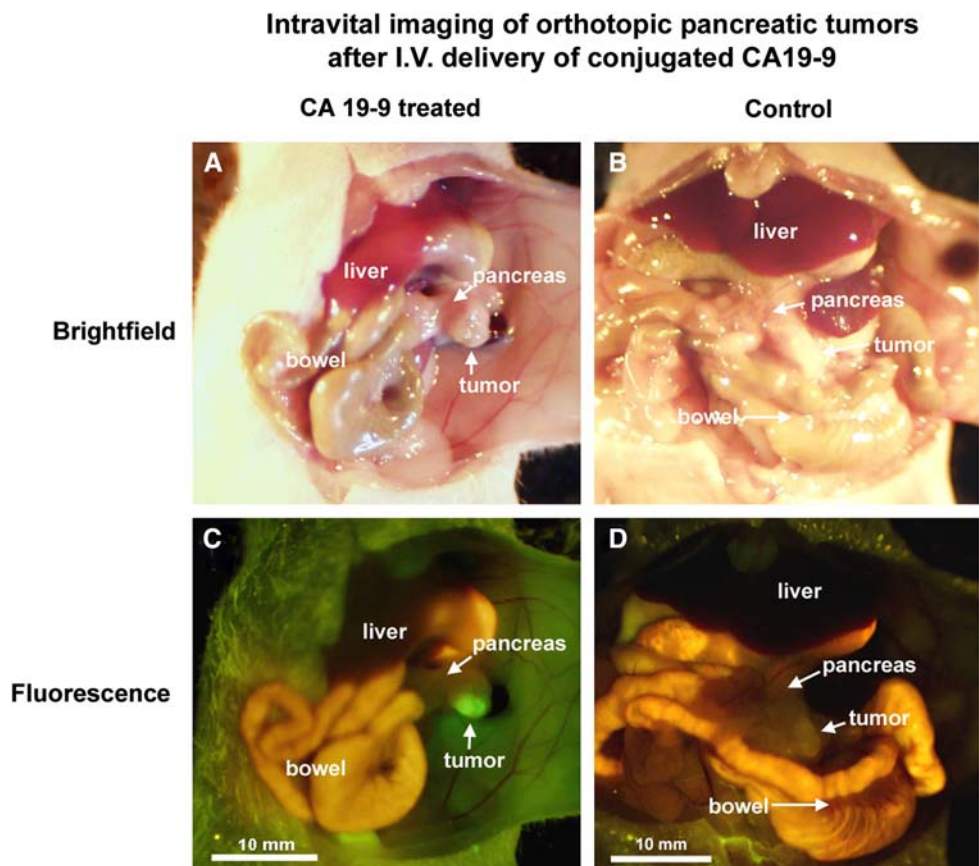


bright-field and fluorescence intravital imaging (Fig. 4B, D).

Conjugated CA19-9 was observed to be bound to tumor cells but not to the surrounding peritumoral stroma by fluorescence histology (Fig. 5). Following laparotomy and whole-body imaging, the orthotopic pancreatic tumors

from animals given a single 75- $\mu$ g IV dose of conjugated CA19-9 were harvested and frozen sections were evaluated after H&E staining using standard bright-field microscopy and without any additional staining via fluorescence microscopy. Both fluorescence microscopy and H&E imaging revealed the characteristic pattern of clusters of

**Fig. 4** Intravital imaging of pancreatic cancer after intravenous delivery of conjugated CA19-9. Two weeks after surgical orthotopic implantation of solid tumor to the pancreas, mice were given a single intravenous dose of 75  $\mu$ g of CA19-9. The animals were anesthetized 24 h later and the tumors within the pancreas were imaged at laparotomy. Small tumors that were indistinguishable from normal adjacent pancreas under bright-field (A) were clearly visible using fluorescence (C). Control animals bearing orthotopic tumors without exposure to conjugated anti-CA19-9 (B) showed low autofluorescence of the primary tumor under fluorescence (D) ( $n = 4$ )



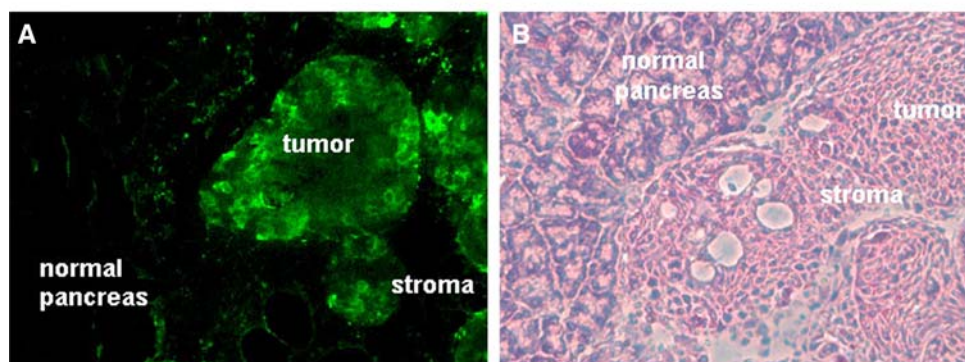
adenocarcinoma cells surrounded by dense peritumoral stroma. Under fluorescence imaging it was apparent that the cancer cells themselves showed a clear green signal with minimal fluorophore present in the adjacent stroma or surrounding pancreas (Fig. 5A). H&E-stained sections demonstrated tumor architecture with clusters of tumor cells surrounded by stromal elements (Fig. 5B, D). In the absence of *in vivo* administration of the fluorophore-conjugated antibody, the orthotopic tumor demonstrated virtually no fluorescence signal (Fig. 5C).

Administration of conjugated CA19-9 facilitated visualization of experimental metastatic implants in the spleen, liver, and peritoneum at laparotomy (Figs. 6-8). Approximately 1-2 weeks following injection of tumor cells, mice were given a single dose of 75  $\mu$ g of conjugated CA19-9. Twenty-four hours after administration of the antibody, the mice were anesthetized and imaged via a midline

laparotomy incision. Microscopic splenic implants that were not visible under bright-field illumination, even at high magnification (Fig. 6A-C), were easily distinguishable from normal splenic tissue using fluorescence imaging (Fig. 6D-F). In the liver, larger metastases were visible using white light illumination. Adjacent smaller implants that could not be seen under bright-field imaging (Fig. 7A-C) were readily visible using fluorescence (Fig. 7D-F). Perhaps most dramatic, tiny peritoneal implants that were impossible to distinguish, even under high bright-field magnification (Fig. 8A), were clearly apparent on the peritoneal surface when imaged under fluorescence (Fig. 8B). Control animals with slightly larger peritoneal implants were visible at high magnification under bright-field microscopy (Fig. 8C), and demonstrated minimal autofluorescence (Fig. 8D). All metastatic lesions in the spleen, liver, and peritoneum were confirmed by histologic

### Fluorescence and H&E imaging of sectioned pancreatic tumors

#### CA19-9 treated



#### Control

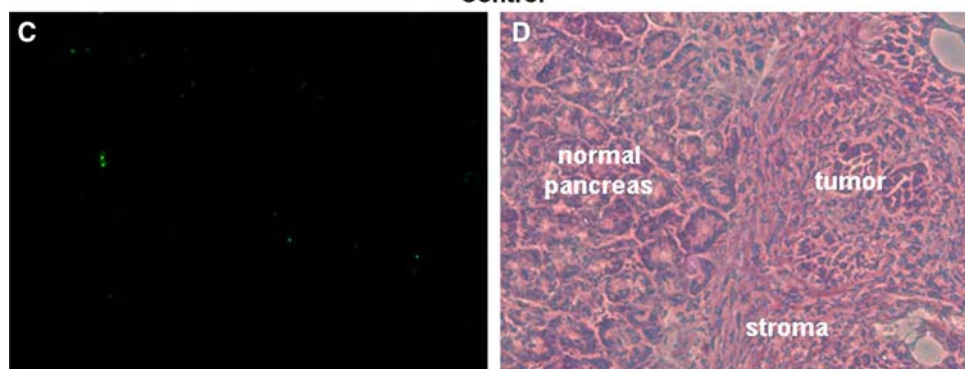


**Fig. 5** H&E and fluorescence imaging of sectioned pancreatic tumors after intravenous delivery of conjugated CA19-9. Following antibody administration, laparotomy, and intravital imaging of orthotopic tumors, the pancreatic tumors were resected en bloc with surrounding normal pancreatic tissue and frozen in OCT for sectioning. Thick (15 mm) sections were evaluated unfixed for green fluorescence and thin (8 mm) sections were prepared by H&E staining. Evaluation of H&E-stained thin sections under standard light

microscopy at 200 $\times$  magnification revealed a characteristic pattern of clusters of tumor cells surrounded by a dense network of stromal cells in all tumors sectioned (**B**, **D**). Fluorescence microscopy of unfixed thick sections under 200 $\times$  magnification revealed a bright green signal from the tumor cells with minimal staining of the surrounding peritumoral stroma (**A**), while a sectioned tumor from a control animal that was not given antibody revealed essentially no fluorescence (**C**) ( $n = 4$ )

## Splenic metastases imaged after I.V. administration of conjugated CA 19-9

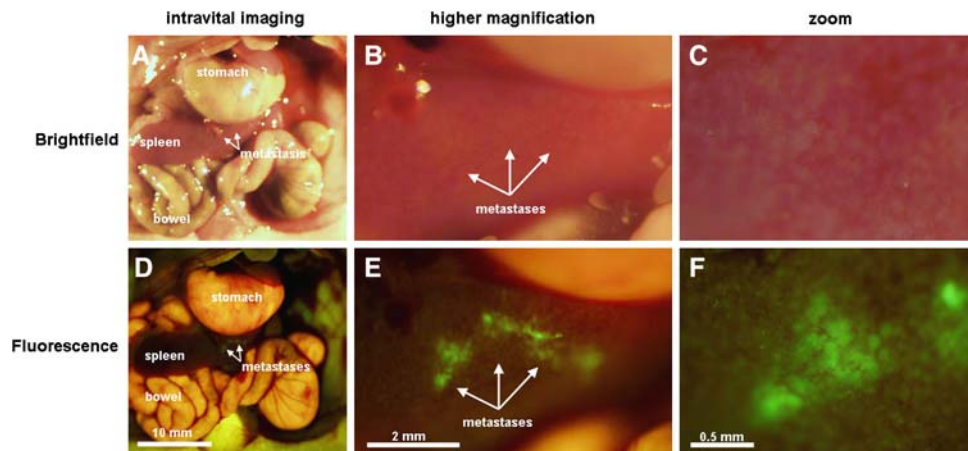


**Fig. 6** Experimental metastatic splenic lesions imaged after intravenous delivery of conjugated CA19-9. Approximately 1 week after direct injection of tumor cells to the spleen, the mice were given a single intravenous dose of 75  $\mu$ g of CA19-9. Twenty-four hours later the animals were anesthetized and evaluated at laparotomy via

evaluation following whole-body imaging (data not shown).

## Discussion

Pancreatic cancer cells are antigenically distinct from other cells in the body. The expression of tumor-associated antigens by these cancer cells provides a unique opportunity for targeted identification of tumor tissue. CA19-9 is a tumor-associated antigen first described in human colorectal cancer in 1979, after development of a monoclonal antibody specific for the human colon cancer line SW 1116 [13]. It is a sialylated Lewis (Le)<sup>a</sup> blood group antigen present in several different gastrointestinal cancers, including that of the colon, stomach, ovary, and pancreas [14–16]. CA19-9 has become the gold standard for serologic testing of patients with pancreatic cancer, and serum levels have been shown to have prognostic value in predicting survival in this patient population [17, 18]. It is important to note that patients who do not express Lewis antigen do not produce CA19-9. The percentage of patients who are Le<sup>a-b-</sup> in the general population is relatively small, ranging from 5% to 15% [19]. Nevertheless, several pathologic studies have evaluated banks of human tumor specimen for CA19-9 expression and have found up to 85–94% of human pancreatic adenocarcinoma tissue samples positive for CA19-9 in unselected groups of patients with pancreatic cancer [8, 20, 21].

It should be noted that *in vitro* testing of several different human tumor cell lines yielded only 3/11 (27%) cell lines that were positive for CA19-9 expression. This was a

intravital imaging using both bright-field and fluorescence imaging. In the spleen, micrometastases, which were indistinguishable from normal tissue under bright-field imaging, even at high magnification (A–C), were clearly visible using fluorescence imaging (D–F)

surprising finding given the high percentage of human pancreatic ductal adenocarcinomas (PDAC) that express CA19-9 on pathologic evaluation [8, 20, 21]. In fact, this low percentage of CA19-9 expression may reflect differences between primary human tumor samples and high-passage human tumor cell lines. It would be expected that the previously-reported pathologic studies of CA19-9 expression in human PDAC specimen would more accurately reflect CA19-9 expression in patients. The human tumor cell line BxPC3 was chosen for our *in vivo* assays because it is a widely used human pancreatic cancer cell line, expresses CA19-9, and shows reliable growth and metastasis in nude mice [9].

Monoclonal antibodies have been used for years in clinical pathology and recently the development of humanized monoclonal antibodies has allowed the safe clinical use of these therapies in patients for the treatment of both solid and hematologic cancers [22]. The natural fluorescence of specific proteins and fluorophore-conjugated antibodies have been used in research for many years [23, 24]. While both of these technologies have been widely available for some time, to date fluorophore-conjugated monoclonal antibodies have not been used in the clinical setting. Two recent animal studies have evaluated the utility of fluorophore-conjugated monoclonal antibodies in the detection of primary and metastatic tumor models [25, 26]. Kulbersh et al. [26] utilized a Cy5.5 fluorophore-conjugated monoclonal antibody specific for epidermal growth factor receptor to improve visualization of orthotopic and subcutaneous human squamous cell carcinoma xenografts in SCID mice. Koyama et al. [25] evaluated the use of rhodamine green-conjugated Herceptin to enhance

**Fig. 7** Metastatic liver lesions imaged after intravenous delivery of conjugated CA19-9. Approximately 2 weeks after implantation of tumor cells to the liver, the mice were given a single intravenous dose of 75  $\mu$ g of CA19-9. Twenty-four hours later the animals were anesthetized and evaluated at laparotomy using both standard white-light illumination and fluorescence imaging. Micrometastases that were indistinguishable from normal tissue under bright-field imaging, even at high magnification (A-C), were clearly visible using fluorescence imaging (D-F)

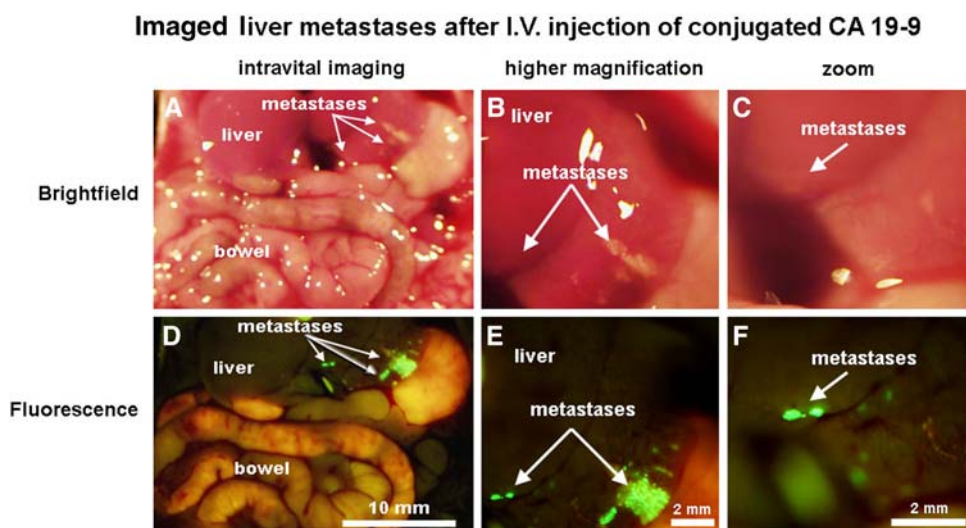
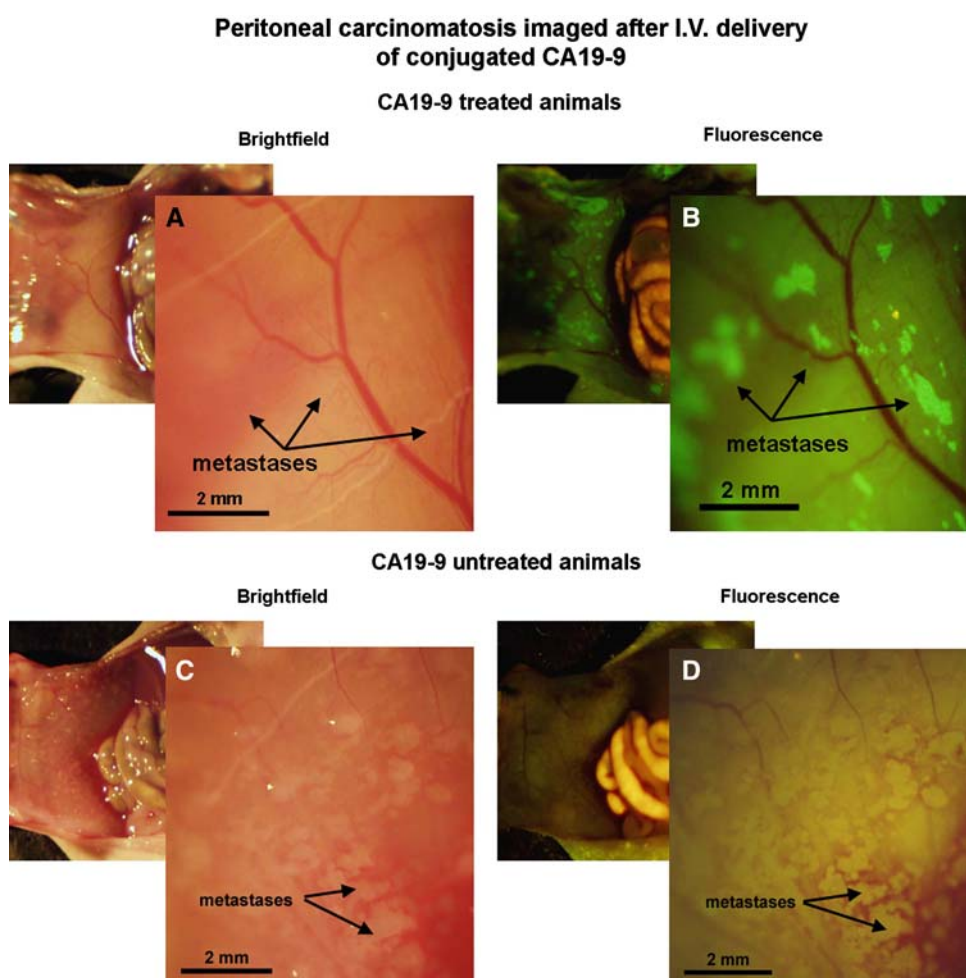


**Fig. 8** Peritoneal tumor implants imaged after intravenous delivery of conjugated CA19-9. Approximately 1 week after injection of tumor cells into the abdominal cavity, mice were given a single intravenous dose of 75  $\mu$ g of CA19-9. Twenty-four hours later the animals were anesthetized and evaluated at laparotomy using both bright-field and fluorescence imaging. Small peritoneal implants that could not be observed, even at the highest magnifications under bright-field imaging (A), were visible when imaged with an LED light source after administration of conjugated antibody (B). Animals with larger peritoneal implants that did not receive the antibody (C) showed minimal autofluorescence of the tumor implants under fluorescence imaging (D)



the localization of Her2/neu gene-transfected murine 3T3 cells in an experimental mouse model of lung metastases. Both groups used in situ postmortem fluorescence imaging and ex vivo tissue analysis and found enhanced ability to locate small tumor implants through the use of targeted

fluorescence technology. In our study we have found similar enhancement of tumor localization at both primary and metastatic sites in living animals via laparotomy and intravital imaging as well as with ex vivo tissue analysis. In our study the mice received a wide range of doses of the

conjugated CA19-9 antibody (from 7.5 to 100  $\mu\text{g}$ ), with successful visualization of the primary tumor at doses ranging from 12.5 to 100  $\mu\text{g}$  per animal, giving a high probability that an effective dose will be found for humans.

Our study used human tumor xenografts within the nude mouse. In humans there is some low-level expression of CA19-9 in normal tissues of the pancreas, but this expression is confined to terminal ductal epithelium and centroacinar cells [7, 27]. In general, staining of these tissues is focal and weaker than those tumors of the pancreas that are positive for CA19-9 expression [27]. Therefore, while nontumor binding of the fluorophore-conjugated CA19-9 antibody may be higher in humans, it is unlikely to be great enough to obscure the signal from the tumor itself. Interestingly, when normal pancreatic tissue from mice treated with conjugated anti-CA19-9 was examined by fluorescence microscopy, a similar staining pattern was observed: Ductal epithelium within the normal pancreatic tissue stained faintly green, with minimal staining of the normal pancreatic tissue (data not shown). This contribution to the background fluorescence was not sufficient to obscure the signal from the tumor during intravital imaging. CA19-9 can also be detected in tissues of the normal human stomach, biliary tract, and bronchial tree, although again, unlike the tumor cells, the staining pattern within normal tissues is typically limited to luminal surfaces [28]. Metastatic tumor implants, even within these tissues would likely have a high signal-to-background ratio because the binding density of the conjugated antibody would be expected to be much greater in the tumor cells themselves.

After intravenous administration of fluorophore-conjugated CA19-9 to tumor-bearing mice, the small primary and metastatic tumor implants, which were difficult to see under bright-field illumination, were clearly distinguishable from background using a fluorescence imaging system. Fluorescent tumors in mice can also be easily visualized, even through the skin, simply by using a small handheld LED (470–480-nm excitation) flashlight [29]. Ideally, a simple handheld fluorescent light source could be used in the operating room during intraoperative staging to facilitate visualization of tumor implants. Alternatively, fluorescence laparoscopy may offer the chance to use this technology to improve staging prior to laparotomy by enhancing visualization of potential metastatic implants within the abdomen. While not every patient with pancreatic cancer will be able to benefit from this technology, surgeons would be able to use fluorophore-conjugated anti-CA19-9 to exploit tumor marker expression in patients with CA19-9 positive pancreatic ductal adenocarcinoma during intraoperative staging. The treatment of tumor implants with sensitizing agents such as 5-aminolevulinic acid followed by fluorescence laparoscopy has been

described in a small number of human subjects, with promising improvement in intraoperative localization of metastatic implants [30]. Our strategy would likewise allow pretreatment of patients to maximize tumor visualization either via fluorescence laparoscopy or with a handheld LED light source at the time of operation.

## Conclusions

We described a new technique designed for surgical navigation in patients with pancreatic cancer. By conjugating a monoclonal antibody specific for the tumor-associated antigen CA19-9 with the AlexaFluor 488 green fluorophore we are able to demonstrate *in vivo* binding of the antibody-fluorophore conjugate to the tumor tissue in a murine model of human pancreatic cancer. This fluorescence not only facilitated differentiation between normal and tumor tissue within the pancreas, it also revealed microscopic foci or tumor implants within the spleen, liver, and peritoneum which were not visible under standard light microscopy. This study shows promising results and offers a novel new technique to facilitate the intraoperative identification of both primary tumor and small metastatic lesions that may be missed at the time of surgery in those patients whose tumors express the tumor-associated antigen CA19-9.

## References

1. Jemal A, Siegel R, Ward E et al (2006) Cancer statistics, 2006. *CA Cancer J Clin* 56(2):106–130
2. Wray CJ, Ahmad SA, Matthews JB et al (2005) Surgery for pancreatic cancer: recent controversies and current practice. *Gastroenterology* 128(6):1626–1641
3. Katz MH, Savides TJ, Moossa AR et al (2005) An evidence-based approach to the diagnosis and staging of pancreatic cancer. *Pancreatology* 5(6):576–590
4. Soriano A, Castells A, Ayuso C et al (2004) Preoperative staging and tumor resectability assessment of pancreatic cancer: prospective study comparing endoscopic ultrasonography, helical computed tomography, magnetic resonance imaging, and angiography. *Am J Gastroenterol* 99(3):492–501
5. Apte MV, Park S, Phillips PA et al (2004) Desmoplastic reaction in pancreatic cancer: role of pancreatic stellate cells. *Pancreas* 29(3):179–187
6. Locker GY, Hamilton S, Harris J et al (2006) ASCO 2006 update of recommendations for the use of tumor markers in gastrointestinal cancer. *J Clin Oncol* 24(33):5313–5327
7. Itzkowitz SH, Yuan M, Fukushi Y et al (1988) Immunohistochemical comparison of Lea, monosialosyl Lea (CA 19–9), and disialosyl Lea antigens in human colorectal and pancreatic tissues. *Cancer Res* 48(13):3834–3842
8. Loy TS, Sharp SC, Andershock CJ et al (1993) Distribution of CA19-9 in adenocarcinomas and transitional cell carcinomas. An immunohistochemical study of 527 cases. *Am J Clin Pathol* 99(6):726–728
9. Bouvet M, Wang J, Nardin SR et al (2002) Real-time optical imaging of primary tumor growth and multiple metastatic events

- in a pancreatic cancer orthotopic model. *Cancer Res* 62(5):1534–1540
10. Katz MH, Bouvet M, Takimoto S et al (2003) Selective anti-metastatic activity of cytosine analog CS-682 in a red fluorescent protein orthotopic model of pancreatic cancer. *Cancer Res* 63(17):5521–5525
  11. Fu X, Guadagni F, Hoffman RM (1992) A metastatic nude-mouse model of human pancreatic cancer constructed orthotopically from histologically intact patient specimens. *Proc Natl Acad Sci USA* 89(12):5645–5649
  12. Yamauchi K, Yang M, Jiang P et al (2006) Development of real-time subcellular dynamic multicolor imaging of cancer-cell trafficking in live mice with a variable-magnification whole-mouse imaging system. *Cancer Res* 66(8):4208–4214
  13. Koprowski H, Stepiewski Z, Mitchell K et al (1979) Colorectal carcinoma antigens detected by hybridoma antibodies. *Somatic Cell Genet* 5(6):957–971
  14. Dede M, Gungor S, Yenen MC et al (2006) CA19-9 may have clinical significance in mature cystic teratomas of the ovary. *Int J Gynecol Cancer* 16(1):189–193
  15. Nozoe T, Rikimaru T, Mori E et al (2006) Increase in both CEA and CA19-9 in sera is an independent prognostic indicator in colorectal carcinoma. *J Surg Oncol* 94(2):132–137
  16. Takahashi Y, Takeuchi T, Sakamoto J et al (2003) The usefulness of CEA and/or CA19-9 in monitoring for recurrence in gastric cancer patients: a prospective clinical study. *Gastric Cancer* 6(3):142–145
  17. Boeck S, Stieber P, Holdenrieder S et al (2006) Prognostic and therapeutic significance of carbohydrate antigen 19-9 as tumor marker in patients with pancreatic cancer. *Oncology* 70(4):255–264
  18. Ferrone CR, Finkelstein DM, Thayer SP et al (2006) Perioperative CA19-9 levels can predict stage and survival in patients with resectable pancreatic adenocarcinoma. *J Clin Oncol* 24(18):2897–2902
  19. Bouvet M (2004) Tumor markers for pancreatic cancer: what happens when preoperative CA 19-9 is undetectable? *Ann Surg Oncol* 11(7):637–638
  20. Haglund C, Lindgren J, Roberts PJ et al (1986) Gastrointestinal cancer-associated antigen CA19-9 in histological specimens of pancreatic tumours and pancreatitis. *Br J Cancer* 53(2):189–195
  21. Yamaguchi K, Enjoji M, Tsuneyoshi M (1991) Pancreatoduodenal carcinoma: a clinicopathologic study of 304 patients and immunohistochemical observation for CEA and CA19-9. *J Surg Oncol* 47(3):148–154
  22. Reichert JM, Valge-Archer VE (2007) Development trends for monoclonal antibody cancer therapeutics. *Nat Rev Drug Discov* 6(5):349–356
  23. Hoffman RM (2005) The multiple uses of fluorescent proteins to visualize cancer in vivo. *Nat Rev Cancer* 5(10):796–806
  24. Paris S, Sesboue R (2004) Metastasis models: the green fluorescent revolution? *Carcinogenesis* 25(12):2285–2292
  25. Koyama Y, Hama Y, Urano Y et al (2007) Spectral fluorescence molecular imaging of lung metastases targeting HER2/neu. *Clin Cancer Res* 13(10):2936–2945
  26. Kulbersh BD, Duncan RD, Magnuson JS et al (2007) Sensitivity and specificity of fluorescent immunoguided neoplasm detection in head and neck cancer xenografts. *Arch Otolaryngol Head Neck Surg* 133(5):511–515
  27. Egami H, Sakamoto K, Yoshimura R et al (1990) Comparative studies on the expression of gastrointestinal-cancer-associated antigen, PA8-15, CA19-9 and the blood-group antigens in non-malignant and malignant human pancreatic tissues. *J Cancer Res Clin Oncol* 116(4):365–371
  28. Dietel M, Arps H, Klapdor R et al (1986) Antigen detection by the monoclonal antibodies CA19-9 and CA125 in normal and tumor tissue and patients' sera. *J Cancer Res Clin Oncol* 111(3):257–265
  29. Yang M, Luiken G, Baranov E et al (2005) Facile whole-body imaging of internal fluorescent tumors in mice with an LED flashlight. *Biotechniques* 39(2):170, 172
  30. Zopf T, Schneider AR, Weickert U et al (2005) Improved pre-operative tumor staging by 5-aminolevulinic acid induced fluorescence laparoscopy. *Gastrointest Endosc* 62(5):763–767